Supplementary Information:

for

"Generalizing, Extending, and Maximizing Nitrogen-15 Hyperpolarization Induced by Parahydrogen in Reversible Exchange"

Johannes F. P. Colell[#], Angus W. J. Logan[#], Zijian Zhou[#], Roman V. Shchepin[†‡], Danila A. Barskiy, Gerardo X. Ortiz Jr.[#], Qiu Wang[#], Steven J. Malcolmson[#], Eduard Y. Chekmenev[†‡], Warren S. Warren[#∂,*], and Thomas Theis[#,*]

Department of Chemistry, Duke University, Durham, NC 27708, USA, †‡ Vanderbilt Institute of Imaging Science (VUIIS), Department of Radiology, Department of Biomedical Engineering, Vanderbilt Ingram Cancer Center (VICC), Vanderbilt University, Nashville, TN 37232, USA; Russian Academy of Sciences, Moscow, Russia, ∂ Departments of Physics, Radiology and Biomedical Engineering, Duke University, Durham, NC 27707, USA.

* Corresponding authors: thomas.theis@duke.edu, warren.warren@duke.edu

Synopsis

This document first provides a discussion of the chemical exchange occurring at Iridium centers in SABRE complexes. At these complexes a sequence of chemical events, is required for polarization buildup on a target nucleus. Next, the document details the determination of average complex lifetime. Then, a theoretical model for the SABRE-SHEATH process is discussed, which results in a simple analytical expression describing magnetic field and temperature dependence of observed enhancements. The expression contains only characteristic *J*-coupling constants in the polarization transfer complex and the average lifetime of the catalytic species. We conclude with detailed information about experimental procedures and spectral data.

Table of Contents

1 Characteristics of SABRE catalysis

Jack Halpern has stated that "catalysis is per definition a kinetic phenomenon".[1] As SABRE is nothing more than a catalytic process, understanding the polarization buildup requires knowledge of the rate constants of the central catalytic pathways.

In SABRE, the polarization source is parahydrogen (*para*-H_2). The *para*-order is consumed when polarization is transferred to nuclei in other substrates, also producing orthohydrogen (*ortho*-H_2) hyperpolarized in one of its triplet states. The postulated catalytic cycle is depicted in Fig. S1. In step 1, *para*-H_2 enters the catalytic cycle by reacting with the short-lived 16-electron complex[2]. This replenishes the polarization source. In the second step, the inserted parahydrogen replaces depleted *ortho*-H_2 which is released in step 3. This replacement of orthohydrogen by parahydrogen only occurs with 50% probability because the depicted $Ir(H)_2(\eta^2\text{-}H_2)$ species have identical energies. In step 4, substrate is incorporated into the 16-electron complex forming the actual polarization transfer species. Notice that the inserted substrate, S, may already carry some hyperpolarization. The polarization transfer species is the most stable and longest lived species in the depicted cycle. Here, equilibration of spin temperature between parahydrogen and substrate takes place. This hyperpolarization transfer/equilibration only takes place at an appropriate magnetic field as detailed in section 3. Closing the cycle, step 6 releases the hyperpolarized substrate. Since all processes are reversible and we rely on an equilibration of polarization, it is critical to constantly refresh the solution with highly enriched para-H_2 at the highest possible rate.

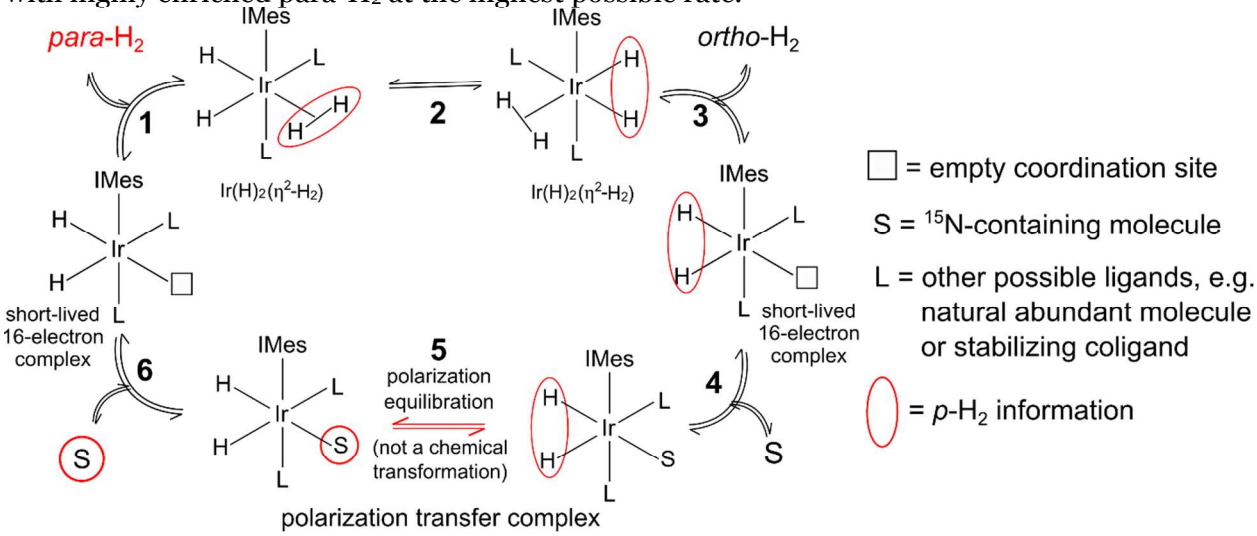

FIGURE S1: The chemical exchange processes leading to polarization buildup on free substrate.

2 Complex Lifetime Determination

To determine the lifetime of the "polarization transfer complex" (see Fig. S1), we monitor the line-broadening observed on the catalyst bound ^{15}N species. The chemical exchange causes this line broadening which can in be used as a measure of the exchange-kinetics.

Each individual data point in the experimental dataset (Fig. 1C, main text) is obtained by bubbling *para*-hydrogen for 90 s at a given temperature [(0, 11, 22, 33 and 44) °C] and a given magnetic field. Then the sample is transferred into the high field magnet for detection and a simple 1D spectrum is acquired.

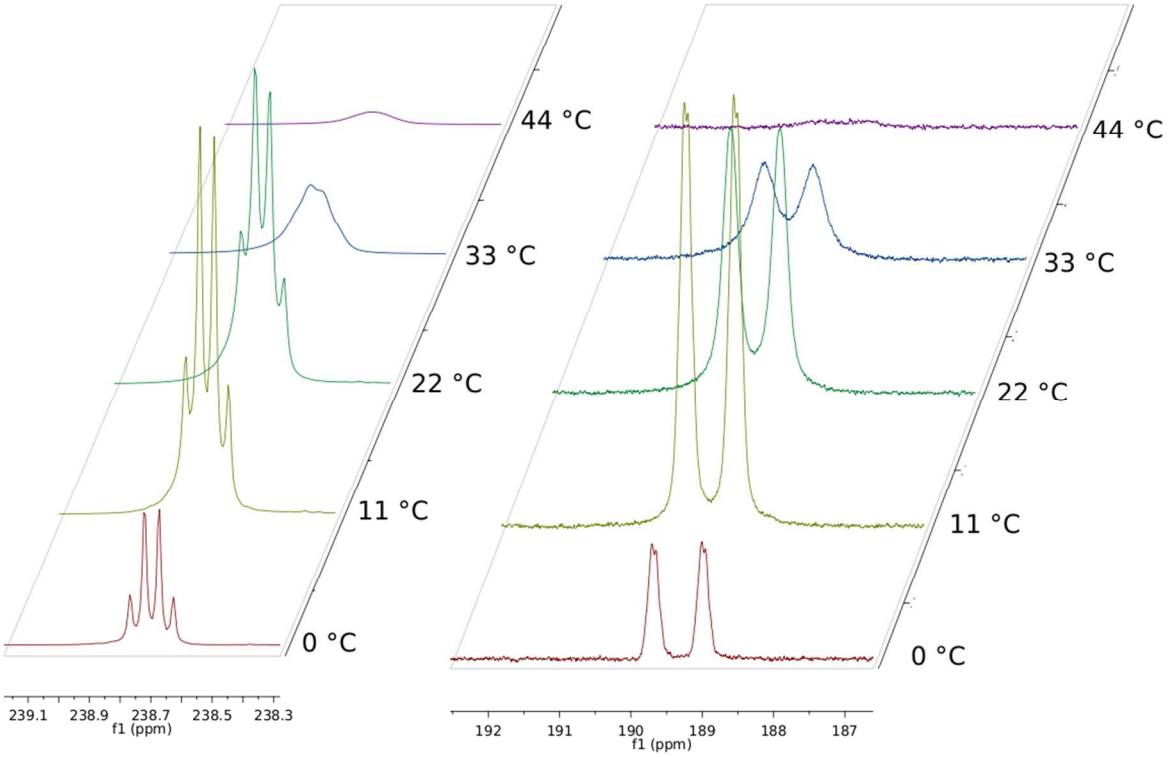

FIGURE S2: Temperature dependence of the ^{15}N SABRE-SHEATH signal intensities for ^{15}N-acetonitrile (100mM). Spectra on the l.h.s. are from the free species. Spectra on the r.h.s. are the bound species and are magnified for clarity. The evolution field (0.9 μT) and evolution time (90 s, polarization is equilibrated at all temperatures within this timeframe and for this substrate) are identical for all temperatures

The lifetime is determined by fitting Lorentzian-Gaussian type functions to both free and bound species. The fundamental uncertainty relation

$$\delta E \delta \tau \geq \tfrac{1}{2}\hbar, \qquad \text{(Eq. S1)}$$

correlates δE the energy uncertainty and $\delta \tau$ the lifetime of a state.

If no additional line broadening mechanism is active the lifetime of the catalyst bound state can be obtained from[3]

$$\delta \tau = \frac{1}{\pi \Delta \nu_{1/2}} \qquad \text{(Eq. S2)}$$

However, inhomogeneous magnetic fields cause additional broadening. The corrected lifetime $\delta \tau_{corr}$ is obtained by subtracting the linewidths of the free species $\Delta \nu_{1/2,free0}$ at 0 °C (which is dominated by the inhomogeneous field effects) from the catalyst bound $\Delta \nu_{1/2,bound}$.

$$\delta \tau_{corr} = \frac{1}{\pi(\Delta \nu_{1/2,bound} - \Delta \nu_{1/2,free0})} \qquad \text{(Eq. S3)}$$

As mentioned in the main article, accurate analysis requires knowledge of characteristic J_{NH}-couplings in the free and catalyst bound ^{15}N acetonitrile and free acetonitrile as well as the hydride to catalyst bound ^{15}N couplings.

As shown in Fig. S3 (also shown as Fig. 2B,C in the main article) at 0°C the relevant *J*-couplings and line positions are directly observable in the ^{15}N and ^{1}H spectra. These values were used as fixed parameters to perform fitting and determine the linewidth $\Delta\nu_{1/2}$.

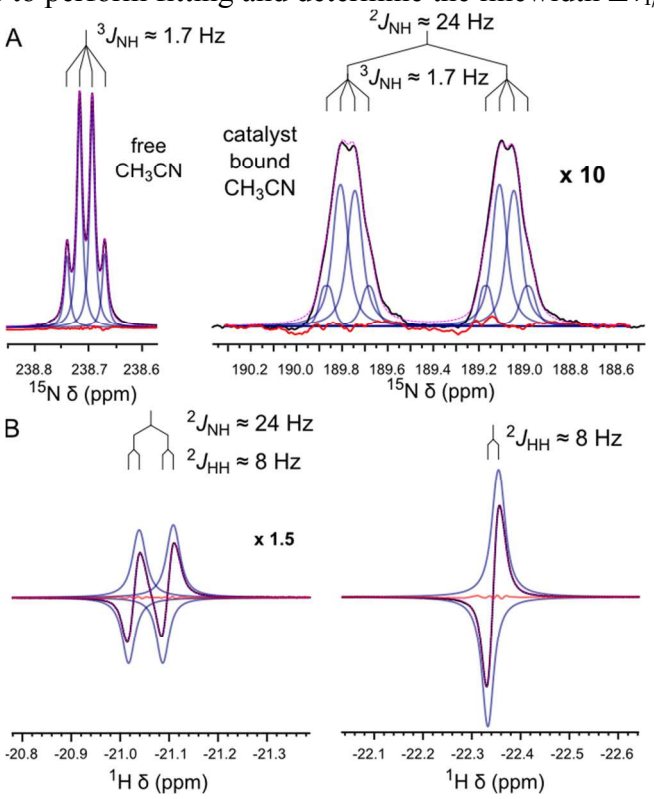

Figure S3: A) Lineshape analysis of ^{15}N spectra used for complex lifetime determination $\tau_{life} \propto 1/k_{diss,Substrate}$ (Blue: individual Lorentzians, black: Experimental trace, Pink: overall fit, red: residual error). The *J*-coupling constants are accessible from the spectra at 0°C, results are shown in Table S1. Spectra from evolution at different temperatures are evaluated to obtain $\tau_{life}(T)$. B) ^{1}H spectra of the hydride region taken under PASADENA conditions.[4] The spectra show $J_{HH'}$ = 8 Hz and ΔJ_{NH} = 24 Hz.

For a spontaneous dissociation (first order chemical reaction)[5-7] we obtain an exponential dependence of rate constant of substrate dissociation, or lifetime for which it remains bound, on the temperature as defined by the Arrhenius Law.

$$\begin{aligned} 1/\tau_{life} &= 1/\tau_0\, e^{-E_A/RT} \\ \Leftrightarrow \tau_{life}(T) &= \tau_0\, e^{E_A/RT} \\ \Leftrightarrow ln\left(\tau_{life}(T)\right) &= ln\,\tau_0 + E_A/RT \end{aligned} \qquad \text{(Eq. S4)}$$

We use this equation to fit our data as shown in Fig. S4 and obtain Arrhenius corrected complex-lifetimes listed in Table S1.

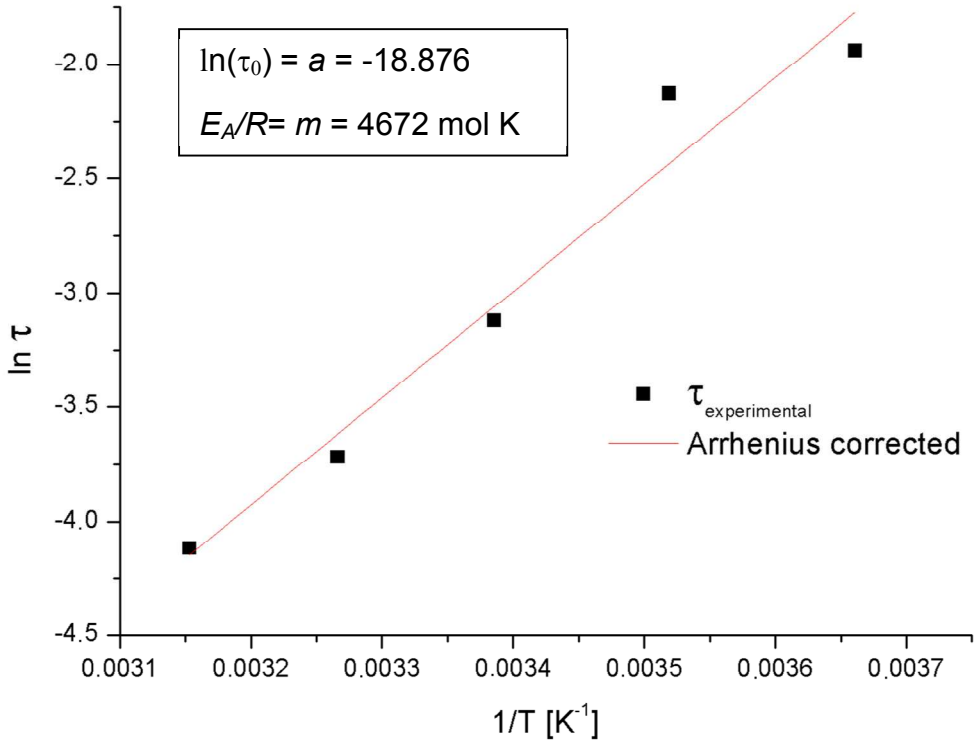

FIGURE S4: Lifetime correction according to Eq. S4. The individual lifetimes are determined by fitting the spectra and analyzing linewidths, which are then converted to lifetimes using Eq. S3.

Table S1: Experimental lifetimes and Arrhenius corrected lifetimes by fitting the data as shown in Fig. S4.

Temperature [°C]	$\Delta\nu_{1/2,bound}$ [Hz]	$\Delta\nu_{1/2,free0}$ [Hz]	Lifetime [s] (Experiment)	Lifetime [s] Arrhenius corrected
0	2.7	0.5	0.143	0.170
11	3.2	-	0.119	0.088
22	7.7	-	0.044	0.047
33	13.6	-	0.024	0.027
44	20.0	-	0.016	0.016

3 Theory

The polarization transfer catalysts used in SABRE have an octahedral coordination environment for Iridium in the polarization transfer step. The polarization source (para-H_2) and substrates occupy equatorial positions (See Fig. S5A). Our theory focuses on the relevant NMR active nuclei: ^{1}H and ^{15}N. Depending on the chemical composition we encounter 3-spin or 4-spin systems (Fig. S5A).When using substrates with ^{15}N at natural abundance (0.37%), or when excess non-labelled coligand is used in conjunction with a ^{15}N enriched substrate, the majority of polarization transfer complexes contains only three NMR active nuclei (two protons, one ^{15}N, left panel of Fig. S5A). When substrates are enriched in ^{15}N (typically >98%) and a maximum of one catalyst-equivalent of unlabelled coligand is present we are largely concerned with the four spin case with two ^{1}H and ^{15}N nuclei (right panel of Fig. S5A). In Fig. S5B we show the spin systems in the well-established Pople syntax[8] (AA'B for naturally abundant ^{15}N-substrates or AA'BB' for labelled ^{15}N-substrates) and introduce the relevant *J*-coupling parameters.

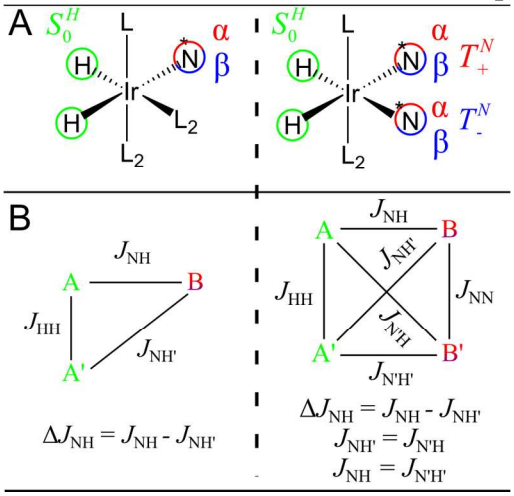

Figure S5: A) The dihydrido substrate complexes with para-H_2 (green) and Nitrogen-15. Note that naturally abundant ^{15}N (or large amounts of unlabeled coligand) gives rise to three-spin system (left), whereas fully ^{15}N enriched substrates result in four-spin systems (right). In low magnetic fields, symmetry and small frequency differences results in an AA'B three-spin system for naturally abundant nuclei and AA'BB' four-spin system for labelled substrates. B) Spin systems and parameter declarations used in the theory.

To understand the polarization transfer driven in these systems we consider the Hamiltonians of the AA'B and the AA'BB' systems. They are expressed in the most convenient basis. For the AA'B system that is a singlet-triplet basis for the AA' pair and the Zeeman basis for the B spin. For the AA'BB' system that is a singlet triplet basis for both AA' and BB' spin pairs.

For completeness, we list both complete Hamiltonians at the end of this theory section. However, because of their apparent complexity at first glance, we introduce a number of simplifications that result in simple analytical expressions for the hyperpolarization transfer. The simplifications are justified by excellent agreement between full simulations and simplified theory. We illustrate the simplification procedure for the AA'B system in Fig. S6 and for the AA'BB' system in Fig. S7.

As illustrated in Fig. S6, the three spin AA'B Hamiltonian (an 8x8 matrix) has two 3x3 and two 1x1 blocks. The four spin Hamiltonian (a 16x16 matrix), divides into two major parts containing either all symmetric states or all anti-symmetric states as can be seen in Fig. S7. The

symmetric part consists of two 1x1 blocks, two 2x2 blocks and one 4x4 block. The anti-symmetric part consists of three 2x2 blocks.[9-10]

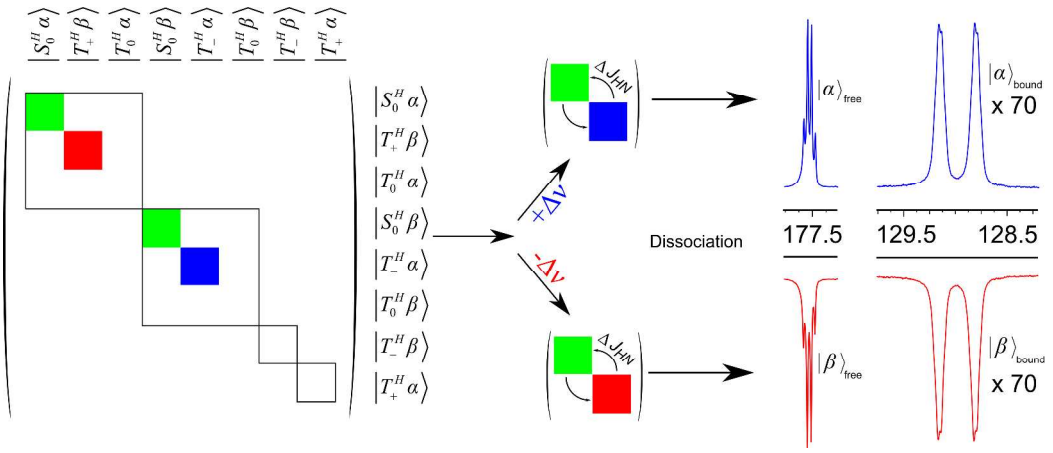

Fig. S6: Left: Representation of the 8x8 Hamiltonian for the AA'B three-spin system. (The full Hamiltonian is given at the end of this section). The Hamiltonian contains two 3x3 blocks that connect the hydrogen singlet initial state (green) and a Zeeman-state for nitrogen which gets hyperpolarized ($|\alpha\rangle$ or $|\beta\rangle$). Middle: Depending on the magnetic field it is possible to selectively overpopulate either $|\alpha\rangle$ or $|\beta\rangle$ nitrogen Zeeman state. Right: Experimental spectra of free and bound 15N-Acetonitrile at the different magnetic field / matching condition.

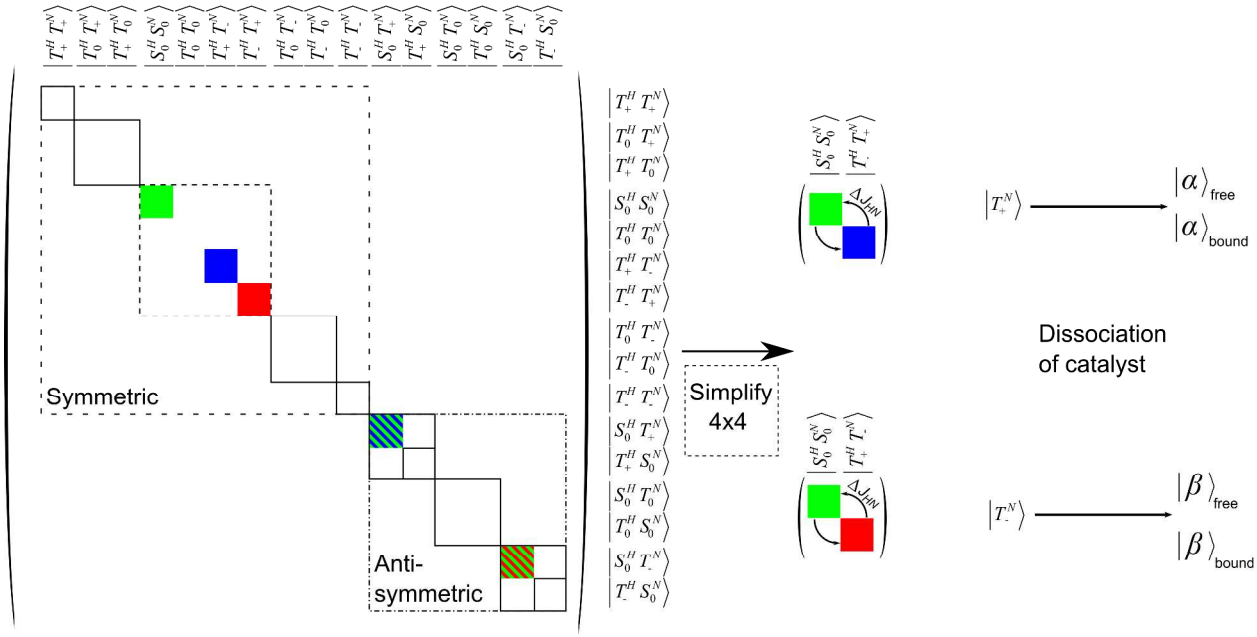

Figure S7: Representation of the 16x16 Hamiltonian for the AA'BB' four-spin system. (The full Hamiltonian is given at the end of this section). Left: The 16x16 matrix with basis states. The relevant matrix elements are the singlet-singlet (green) and its connections to the possible triplet-triplet states (blue and red). Middle: Reduced submatrices with singlet to $|T_-^N\rangle = |\beta\beta\rangle$ and $|T_+^N\rangle = |\alpha\alpha\rangle$ connections treated in the theory. Fulfilling the matching condition for $|T_+^N\rangle = |\alpha\alpha\rangle$ state

will result in in-phase magnetization) for free and bound hyperpolarized species. Targeting $|T_-^N\rangle = |\beta\beta\rangle$ yields signal with opposite phase.

As para-hydrogen is the polarization source we first identify the states containing the para-hydrogen singlet out of the 8 or 16 states of the three- and four-spin systems. They are marked green in Fig. S6 and Fig. S7. Hyperpolarization is the process of building up a significant amount of excess $|\alpha\rangle$ or $|\beta\rangle$ polarization. We are thus interested in identifying the blocks of the Hamiltonian that connect hydrogen singlets and Nitrogen $|\alpha\rangle$ or $|\beta\rangle$ Zeeman states (or equivalently $|T_+^N\rangle$ or $|T_-^N\rangle$ nitrogen triplet states for the four-spin case) marked in blue and red in Figs. S6 and S7.

We find that all such blocks are similar in structure and we represent all the identified 2x2 connections in the three spin case as

$$H = 2\pi \begin{array}{c} \begin{matrix} |S_0(^1H)\rangle & |\alpha \text{ or } \beta(^{15}N)\rangle \end{matrix} \\ \begin{pmatrix} -\left(J_{HH} + \frac{\Sigma J_{NH}}{4}\right) & \frac{\Delta J_{NH}}{4} \\ \frac{\Delta J_{NH}}{4} & (+-)\ \Delta\nu_{HN} \end{pmatrix} \end{array} \begin{array}{l} |S_0(^1H)\rangle \\ |\alpha \text{ or } \beta(^{15}N)\rangle \end{array} \qquad \text{(Eq. S5)}$$

where $\Delta\nu_{HN} = (\nu_H - \nu_N)$, $\Delta J_{NH} = J_{NH} - J_{NH'}$ and $\Sigma J_{NH} = J_{NH} + J_{NH'}$.

If the diagonal elements within this block are equal, hyperpolarization can be transferred from a para-hydrogen singlet either to $|\alpha\rangle$ or $|\beta\rangle$ population, depending on the direction of the magnetic field. The driving force of the hyperpolarization transfer are the off-diagonal elements $\propto J_{\mathrm{NH}}$. Optimal polarization transfer is established on resonance when the diagonal elements are the same. These insights shed light on the conditions for hyperpolarization transfer in the absence of exchange. By setting the diagonal elements equal to each other we derive Eq. 1 of the main manuscript.

$$\Delta\nu_{HN} = \pm\left(J_{HH} + \frac{\Sigma J_{NH}}{4}\right), \qquad \text{(Eq. S6)}$$

when solved for the magnetic field using $\Delta\nu = (\gamma_H - \gamma_N)B_{evo}$ we obtain

$$B_{evo} = \pm\frac{J_{HH} + \frac{\Sigma J_{NH}}{4}}{(\gamma_H - \gamma_N)} \qquad \text{(Eq.S7)}$$

identical to Eq. 1 in the main manuscript.

To analyze the dynamics in more detail we begin with an initial state containing pure hydrogen singlet and formulate the initial density matrix right after inserting a new para-hydrogen molecule into the polarization transfer complex as:

$$\rho(0) = \begin{array}{c} \begin{matrix} |S_0(^1H)\rangle & |\alpha \text{ or } \beta(^{15}N)\rangle \end{matrix} \\ \begin{pmatrix} 1 & 0 \\ 0 & 0 \end{pmatrix} \end{array} \begin{array}{l} |S_0(^1H)\rangle \\ |\alpha \text{ or } \beta(^{15}N)\rangle \end{array} \qquad \text{(Eq. S8)}$$

which is propagated with the Hamiltonian of Eq. S5 as

$$\rho(t) = e^{iHt}\ \rho(0)\ e^{-iHt} \qquad \text{(Eq. S9)}$$

We are primarily interested in the ρ_{22} matrix element of $\rho(t)$ because it describes the population p of the nitrogen Zeeman-states $|\alpha\rangle$ or $|\beta\rangle$ (or the $|T_-^N\rangle = |\beta\beta\rangle$, $|T_+^N\rangle = |\alpha\alpha\rangle$ in the four spin case).

We obtain

$$p(\alpha) = \frac{sin\left(\frac{\pi}{2} t\sqrt{\Delta J_{NH}^2 + 4\left(J_{HH} + \Sigma J_{NH}/4 - \Delta\nu_{HN}\right)^2}\right)^2}{1 + 4\left(J_{HH} + \Sigma J_{NH}/2 - \Delta\nu_{HN}\right)^2 / \Delta J_{NH}^2},$$
$$p(\beta) = \frac{sin\left(\frac{\pi}{2} t\sqrt{\Delta J_{NH}^2 + 4\left(J_{HH} + \Sigma J_{NH}/2 + 2\pi\Delta\nu_{HN}\right)^2}\right)^2}{1 + 4\left(J_{HH} + \Sigma J_{NH}/4 + \Delta\nu_{HN}\right)^2 / \Delta J_{NH}^2}. \quad \text{(Eq. S10)}$$

Note that the effective measureable polarization or net magnetization is given as $p(\alpha)$ - $p(\beta)$.

Next, we need to account for the chemical kinetics in the exchange process. This is accomplished by weighting the evolution of populations $p(\alpha)$ and $p(\beta)$ with an exponential lifetime distribution and integrating over time.

$$hp(\alpha) = \frac{1}{\tau_{life}^2}\int_0^\infty p(\alpha) e^{-\frac{t}{\tau_{life}}} dt \quad \text{and} \quad hp(\beta) = \frac{1}{\tau_{life}^2}\int_0^\infty p(\beta) e^{-\frac{t}{\tau_{life}}} dt \quad \text{(Eq. S11)}$$

Note, the division by τ_{life}^2 results from 1) normalization with $\int_0^\infty e^{-\frac{t}{\tau_{life}}} dt = \tau_{life}$ and 2) to account for the number of turnovers the catalyst performs per unit time. In other words, weighting is performed to account for the fact that longer lifetimes are associated with fewer turnovers.

This model assumes that the process is limited only by substrate dissociation, hydrogen replenishment is instantaneous in this model.

Evaluating the integrals of Eq. S11 yields

$$hp(\alpha,\beta) = \frac{\pi^2 \tau_{life} \frac{\Delta J_{NH}^2}{2}}{1 + \pi^2 \tau_{life}^2 \left(\Delta J_{NH}^2 + 4\left(J_{HH} + \Sigma J_{NH}/4(-+)\Delta\nu_{HN}\right)^2\right)}, \quad \text{(Eq. S12)}$$

Finally, the observable net hyperpolarization is the difference of the two:

$$hp = a\left(\frac{2\pi^2 \tau_{life}\ \Delta J_{NH}^2}{1 + 4\pi^2 \tau_{life}^2 \left(\Delta J_{NH}^2 + \left(J_{HH} + \Sigma J_{NH}/4 - \Delta\nu_{HN}\right)^2\right)} - \frac{2\pi^2 \tau_{life}\ \Delta J_{NH}^2}{1 + 4\pi^2 \tau_{life}^2 \left(\Delta J_{NH}^2 + \left(J_{HH} + \Sigma J_{NH}/4 + \Delta\nu_{HN}\right)^2\right)}\right) \quad \text{(Eq. S13)}$$

where *a* is a scaling factor related to the hydrogen exchange rate, solubility, diffusion etc.

The expression of Eq. S13 is fit to our experimental data where we use *a* and τ_{life} as fitting parameters. The *J*-coupling parameters were read from the spectra in Fig. S3 as $\Delta J_{NH} = 24Hz$, ΣJ_{NH} =24 Hz (i.e. J_{NH}=24 Hz, J'_{NH}=0), and J_{HH} =8 Hz.

Table S2: Comparison of experimental lifetimes and theoretical lifetimes.

Temperature [°C]	Lifetime [s] (Experiment)	Lifetime [s] Arrhenius corrected	Lifetime [s] from fitting analytical expression
0	0.143	0.170	0.0092
11	0.119	0.088	0.0045
22	0.044	0.047	0.0038
33	0.024	0.027	0.0015
44	0.016	0.016	0.0011

Inspection of Table S2 reveals that there is currently a sizeable (factor 10 to 20) mismatch between experimental and theoretical lifetimes. Still, the qualitative agreement is good and we are currently investigating causes of this mismatch. In particular, we imagine that pseudo rotation of the hydrides may cause fast exchange between the two hydride sites. This effect would stop the coherent evolution of the polarization transfer; however, the linewidths in the spectra would remain unaffected. If the pseudorotation/hydride-site exchange is about 10 to 20 times faster than the actual ligand exchange, this would explain the mismatch and be consistent with the spectral data.

Hamiltonians in explicit matrix-form:

Hamiltonian for the AA'B system:

$$H_{AA'B} = \begin{array}{c} \\ |S_0\alpha\rangle \\ |T_+\beta\rangle \\ |T_0\alpha\rangle \\ |S_0\beta\rangle \\ |T_-\alpha\rangle \\ |T_0\beta\rangle \\ |T_+\beta\rangle \\ |T_-\alpha\rangle \end{array} \begin{array}{c} \begin{array}{cccccccc} |S_0\alpha\rangle & |T_+\beta\rangle & |T_0\alpha\rangle & |S_0\beta\rangle & |T_-\alpha\rangle & |T_0\beta\rangle & |T_-\beta\rangle & |T_+\alpha\rangle \end{array} \\ \begin{pmatrix} -J_{HH}+\nu_N & \frac{\Delta J_{NH}}{2\sqrt{2}} & -\frac{\Delta J_{NH}}{4} & 0 & 0 & 0 & 0 & 0 \\ \frac{\Delta J_{NH}}{2\sqrt{2}} & \nu_H-\frac{\Sigma J_{NH}}{4} & \frac{\Sigma J_{NH}}{2\sqrt{2}} & 0 & 0 & 0 & 0 & 0 \\ -\frac{\Delta J_{NH}}{4} & \frac{\Sigma J_{NH}}{2\sqrt{2}} & \nu_N & 0 & 0 & 0 & 0 & 0 \\ 0 & 0 & 0 & -J_{HH} & -\frac{\Delta J_{NH}}{2\sqrt{2}} & \frac{\Delta J_{NH}}{4} & 0 & 0 \\ 0 & 0 & 0 & -\frac{\Delta J_{NH}}{2\sqrt{2}} & -\nu_H+\nu_N-\frac{\Sigma J_{NH}}{4} & \frac{\Sigma J_{NH}}{2\sqrt{2}} & 0 & 0 \\ 0 & 0 & 0 & \frac{\Delta J_{NH}}{4} & \frac{\Sigma J_{NH}}{2\sqrt{2}} & 0 & 0 & 0 \\ 0 & 0 & 0 & 0 & 0 & 0 & -\nu_H+\frac{\Sigma J_{NH}}{4} & 0 \\ 0 & 0 & 0 & 0 & 0 & 0 & 0 & +\nu_H+\nu_N+\frac{\Sigma J_{NH}}{4} \end{pmatrix} \end{array}$$

Hamiltonian for the AA'BB' spin system in the AA' singlet-triplet BB' singlet -triplet basis. Note that the order of the basis states is slightly different from the representation of Fig S7.

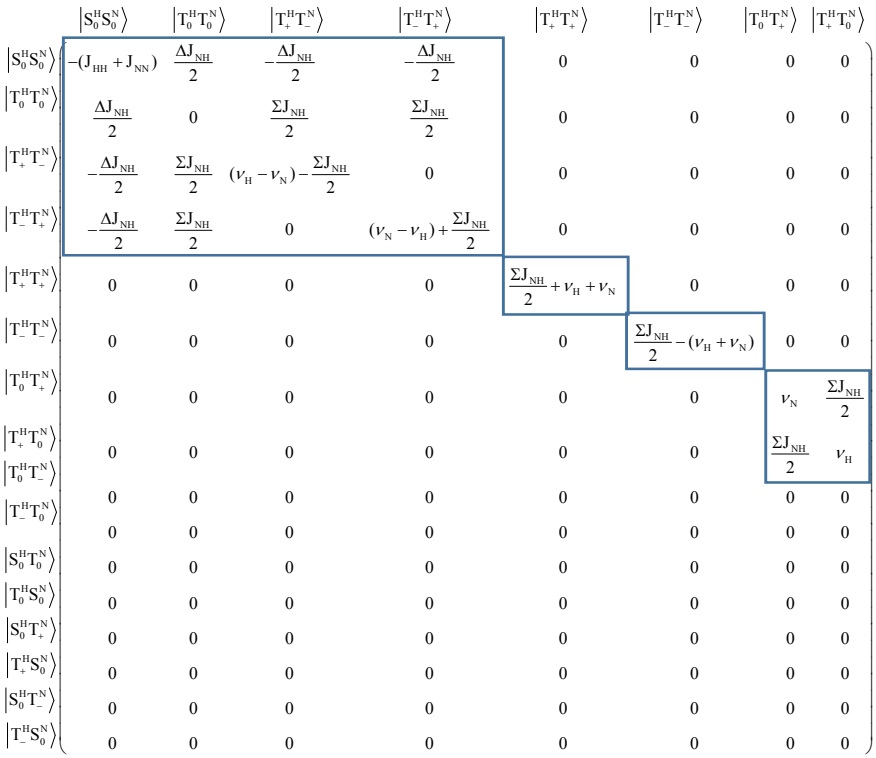

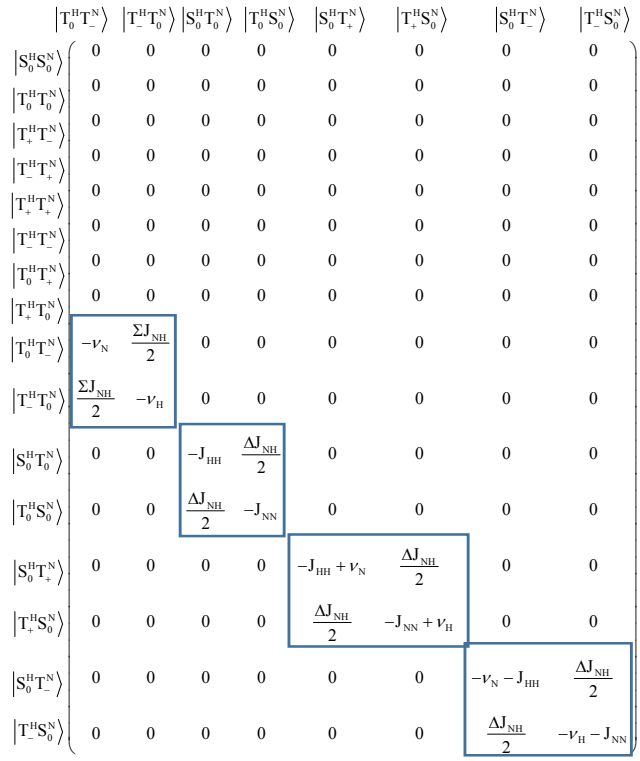

4 Experimental details

The precatalyst **[**Ir(COD)(IMes)]Cl is synthesized in house using published procedures[11-12]. Naturally abundant nitriles and pyridine were purchased at Sigma-Aldrich, isotopically labelled solvents and $^{15}N_5$ Adenine HCl from Cambridge Isotope Laboratories. All compounds were used without further purification. For experiments in MeOH-d4 an appropriate volume of stock solution of precatalyst [IrIMesCOD]Cl is added to substrate and dissolved in MeOH-d4. For neat samples the catalyst is directly dissolved in the substrate of choice. If required, an appropriate volume of pyridine is added to stock solution or sample. In all cases the precatalyst is reacted with para-hydrogen for 20 -100 minutes to obtain the catalytically active species. The activation period is monitored by ^{1}H spectroscopy and intermediate ^{15}N SABRE-SHEATH spectra. Constant ^{15}N-signal integrals are used as a measure of complete catalyst activation.

For SABRE SHEATH measurements the sample is placed inside a solenoid coil within a half-open three layer µ-metal magnetic shield as displayed in Fig. S8. The solenoid coil, series-connected with a shunt resistor, is supplied with adjustable voltage. Current is given by Ohm's law $U/R = I$ and the evolution field $B_{evo} \propto I$. The sample is supplied with para-hydrogen for a time t_{evo} at a given magnetic field B_{evo} and transferred to high field for detection. Signal intensities are influenced by T_1 relaxation, the delay time (transfer time + acquisition start) is 8 s (for 8.45 T) and 3-5 s (for 1T). Sample temperature during evolution was adjusted with a large volume water bath.

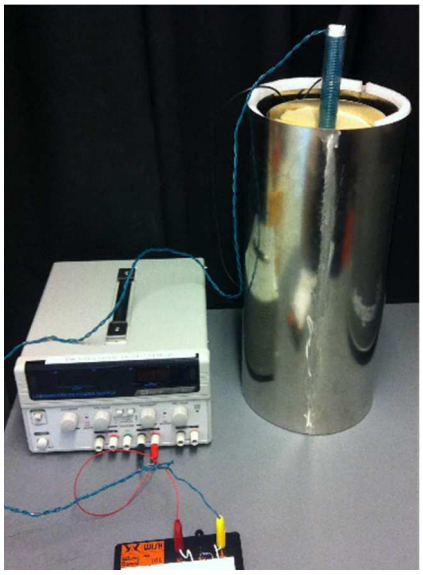

FIGURE. S8: Experimental SABRE-SHEATH setup. The magnetic shields have a shielding factor of ~1000. Fields between 0.5 mG and 130 mG can be adjusted by passing a small current through a solenoid within the shields.

4.1 Additional Data on ^{15}N-Nitrile hyperpolarization

^{15}N-Nitriles can be successfully hyperpolarized in very different molecules and appear to be a good substrate for 15N hyperpolarization in general. This is true for 15N enriched compounds and compounds with 15N at natural abundance as illustrated in Table S3.

Table S3. Signal Enhancements for various nitriles under differing concentration of coligand, (L = pyridine, measured in catalyst equivalents relative to $c_{catalyst}$).

Substrate	$c_{Nitrile}$ [mM]	$c_{Catalyst}$ [mM]	L [catalyst equivalents]	Enhancement
	91	4.0	1	21,000
	neat	4.0	0	700
	100	6.25	5.3	4,300
	neat	4.0	0	600
	91	4.0	1	11,000
	91	4.0	1	3,600

4.2 Small Pulse angle T1 measurements:

For small pulse angle measurements pulse length and power was adjusted to 6° pulses. The sample was hyperpolarized by exposure to para-hydrogen bubbling for 300s at a matching field of 0.6 μT. The sample was transferred to the Magritek 1 T (3 s) or Bruker Avance 400 (8s). Data was obtained by successive application of small pulses.

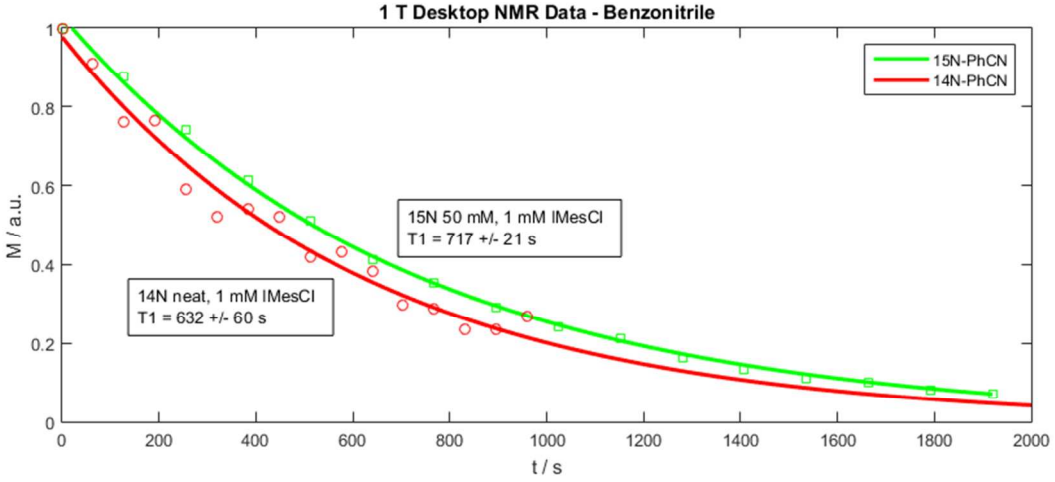

FIGURE S9: Small pulse angle T_1 measurement of 15N relaxation times in neat Benzonitrile with naturally abundant ^{15}N (red) and a 50 Mm solution of 15N labelled Benzonitrile in MeOH-d4.

In Table S4 we provide more detailed information about sample composition and their effects on T1 times at two magnetic fields.

Table S4: T_1 data and experimental conditions:

Compound	[Substrate]	[Catalyst]	Pyridine Additive	T_1 (8.5 T) [s]	Error [s]	T_1 (1 T) [s]	Error [s]
15N Pyridine	50 mM	1mM	N/A	63.0	0.6	124	8
15N Acetonitrile	50 mM	1 mM	yes	123.3	0.3	124	3
14 N Acetonitrile	neat	1 mM	no	131.0	2.5	132	23
14N Acetonitrile d3	neat	1mM	no	142.1	1.6	82	6
14N Pyridine	neat	5 mM	N/A	89.8	2.6	199	18
14N Pyridine d5	neat	5 mM	N/A	95.2	1.0	221	27
15N Diazirine	50 mM	1 mM	yes	9.76	0.12	261	6
14N Benzonitrile	neat	1mM	no	172.6	1.9	632	60
15N Benzonitrile	50 mM	1 mM	yes	129	0.8	717	21

Figure S10 shows the simple benchtop setup: SABRE-SHEATH next to 1T-^{15}N-spectrometer. The experimental procedure is best seen from the supplemental video.

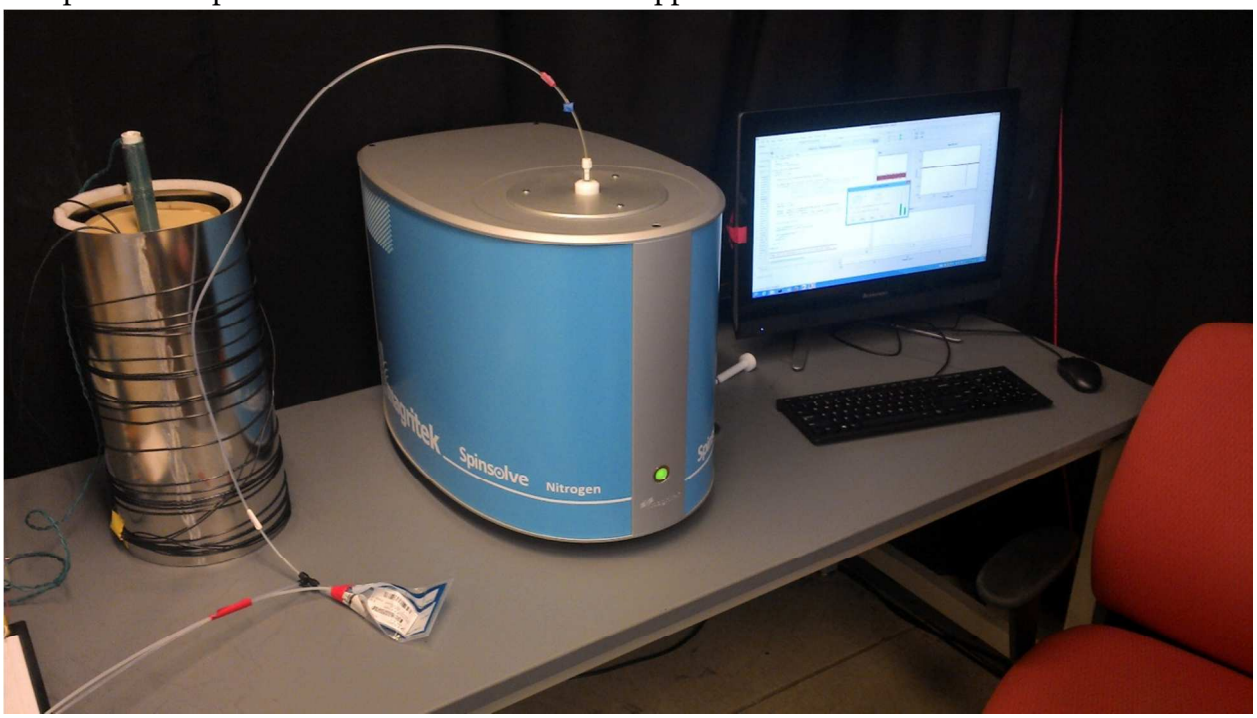

FIGURE S10: The experimental setup for the 1T experiments.

5) Spectral data and miscellaneous information

Following IUPAC recommendations[13] chemical shifts of ^{15}N are referenced on the Ξ-scale (Xi-scale) utilizing the absolute frequency of the d4-methanol quintet (e.g. 360.1300150 mHz) and Ξ_N = 10.1329118 for liquid ammonia to obtain an absolute frequency for 0 ppm[14]. Spectra were acquired on a Bruker Avance 360 (8.45 T) or Magritek Spinsolve Nitrogen 1T. Data was processed with Mestrelab Mnova 8.0.1-10878.

<u>^{15}N-Acetonitrile: Temperature Measurements</u>

^{15}N-NMR (36 MHz, [D4]MeOH, CD_2HOD, 0 °C): δ = 238.7 (q, $^3J(N,H)$ = 1.7 Hz), 189.9 (q, $^3J(N,H)$ = 2.2 Hz), 189.3 ppm (q, $^3J(N,H)$ = 2.3 Hz);
^{15}N-NMR (36 MHz, [D4]MeOH, CD_2HOD, 11 °C): δ = 238.7 (q, $^3J(N,H)$ = 1.7 Hz), 190.0 (d), 189.3 ppm (d);
^{15}N-NMR (36 MHz, [D4]MeOH, CD_2HOD, 22 °C): δ = 238.7 (q, $^3J(N,H)$ = 1.7 Hz), 190.0 (s), 189.3 ppm (s);
^{15}N-NMR (36 MHz, [D4]MeOH, CD_2HOD, 33 °C): δ = 238.7 (d), 190.0 (s), 189.3 ppm (s);
^{15}N-NMR (36 MHz, [D4]MeOH, CD_2HOD, 44 °C): δ = 238.7 (s), 190.0 (s), 189.3 ppm (s).

<u>15N5-Adenine</u>

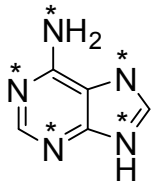

^{15}N-NMR (36 MHz, [D4]MeOH, CD_2HOD, 22 °C): δ = 223.0 (dd, *J* = 5.3 Hz, *J* = 15.2 Hz), 219.2 (dd, *J* = 4.4 Hz, (*J* = 14.4 Hz), 216.4 (d), 165.6 (s), 70.6 (s) ppm.

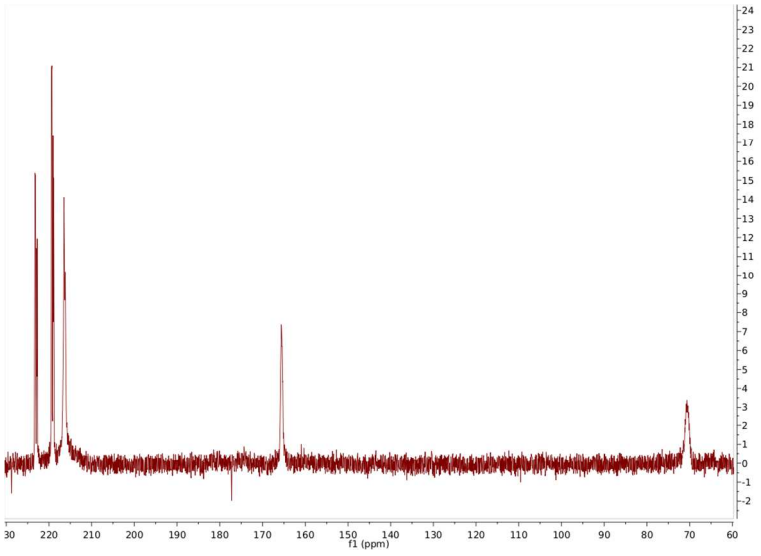

FIGURE S11: SABRE SHEATH spectrum of 15N5-Adenine Hydrochloride neutralized with trimethylamine (pH = 6).

15N2-3,6-Dichloropyridazine

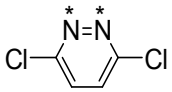

^{15}N-NMR (36 MHz, [D4]MeOH, CD_2HOD, 22 °C): δ = 380.8 (s).

Benzonitrile

^{15}N-NMR (36 MHz, [D4]MeOH, CD_2HOD, 22 °C): δ = 250.1 (s) ppm.

15N2-E/Z-Diphenyldiazine

^{15}N-NMR (36 MHz, [D4]MeOH, CD_2HOD, 22 °C): δ = 522.0 (s), 509.3 (d, $^1J_{NN}$ = 19.2 Hz), 503.5 (s), 424.4 (dd, $^1J_{NN}$ = 19.2 Hz , □J_{NH} = 25.4 Hz) ppm.

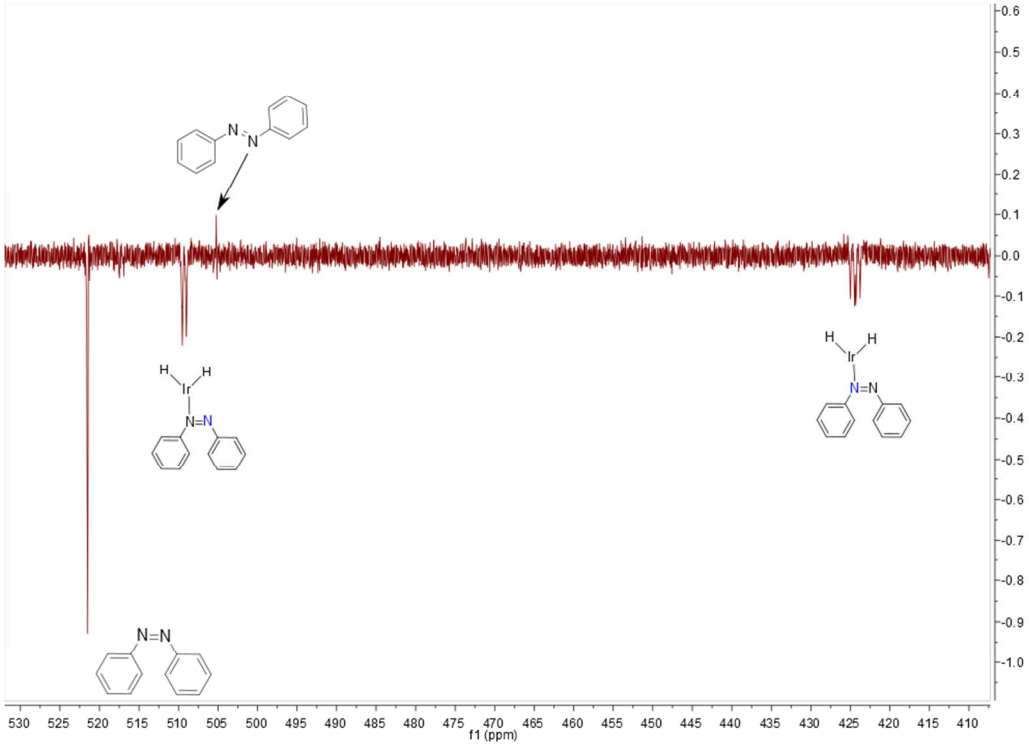

FIGURE S12: Spectrum of E/Z-diphenyldiazene shows free E and free Z species due to short T_1 and high concentration. The nitrogen atom attached to the iridium center has a chemical shift of 80 ppm to the free thermodynamically stable Z-form which is not enhanced. The doublet at 509 ppm is caused by the chemical shift difference between the nitrogen atoms upon single attachment. Note the in-phase peak at 503.5 ppm from thermally polarized E-diphenyldiazene, the evolution field has been deliberately chosen for hyperpolarized compounds to be anti-aligned with residual thermal signal.

This case is especially interesting, as we observe a complex spectral structure. The data indicates a single nitrogen attachment to the catalyst, inducing a chemical shift difference between the otherwise equivalent nitrogens. Binding to the Iridium induces *Z/E* conversions resulting in desorption of free *E*-species. The T_1 relaxation time is extremely short (~1 s) ($c_{Substrate}$ = 91 mM, $c_{Catalyst}$ = 4 mM), a thermal reference could be taken with recycle delay of only 3 s. A thermal

reference with 200000 scans did not show the free *E*-species, therefore enhancement could not be determined accurately and we report that at least a 40 fold enhancement is obtained.

4-hydroxy-α-cyanocinnamicacid (unlabeled)

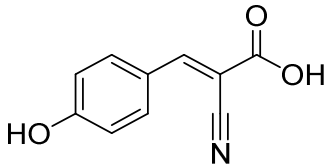

^{15}N-NMR (36 MHz, [D4]MeOH, CD_2HOD, 22 °C): δ = 264.3 (s) ppm.

15N-4-hydroxy-α-cyanocinnamicacid

^{15}N-NMR (36 MHz, [D4]MeOH, CD_2HOD, 22 °C): δ = 264.3 (s), 198.7 (dd, J = 7.2 Hz, J = 30.0 Hz) ppm.

15N2-Diazirine

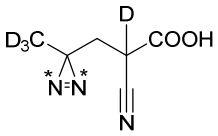

^{15}N-NMR (36 MHz, [D4]MeOH/D_2O 9/1, CD_2HOD, 22 °C): δ = 261.7 (d, $^1J_{NN}$ = 17.3 Hz), 262.5 (d, $^1J_{NN}$ = 17.3 Hz) ppm.

This spectrum has been taken with very narrow spectral range, Nitrile group enhancements are unknown. It is important to note that the chiral carbon position induces a diastereotopic chemical shift between the nitrogen positions. We have observed long lived singlet states in the Diazirine-moiety with relaxation time constants of over 20 min in low magnetic fields.[15] Other aliphatic diazirines with C5-backbones have been investigated and polarize consistently well.

Alectinib

^{15}N-NMR (36 MHz, [D4]MeOH/D_2O 9/1, CD_2HOD, 22 °C): δ = 260.3 (s).

Solubility is poor, no bound resonances visible.

Schiff bases, Nicotinamide, Metroindazole, Imidazole

The reader is referred to Refs. [16-19] for spectral data.

References

1. Halpern, J., Mechanistic aspects of homogeneous catalytic hydrogenation and related processes. *Inorganica Chim. Acta* **1981,** *50*, 11-19.
2. Cowley, M. J.; Adams, R. W.; Atkinson, K. D.; Cockett, M. C. R.; Duckett, S. B.; Green, G. G. R.; Lohman, J. A. B.; Kerssebaum, R.; Kilgour, D.; Mewis, R. E., Iridium N-Heterocyclic Carbene Complexes as Efficient Catalysts for Magnetization Transfer from para-Hydrogen. *J. Am. Chem. Soc.* **2011,** *133*, 6134-6137.
3. Günther, H., *NMR Spectroscopy: Basic Principles, Concepts and Applications in Chemistry*. 3 ed.; Wiley-VCH: Weinheim, Germany, 2013.

4. Bowers, C. R.; Weitekamp, D. P., Transformation of Symmetrization Order to Nuclear-Spin Magnetization by Chemical Reaction and Nuclear Magnetic Resonance. *Phys. Rev. Lett.* **1986,** *57*, 2645-2648.
5. Cowley, M. J.; Adams, R. W.; Atkinson, K. D.; Cockett, M. C. R.; Duckett, S. B.; Green, G. G. R.; Lohman, J. A. B.; Kerssebaum, R.; Kilgour, D.; Mewis, R. E., Iridium N-Heterocyclic Carbene Complexes as Efficient Catalysts for Magnetization Transfer frompara-Hydrogen. *J. Am. Chem. Soc.* **2011,** *133*, 6134-6137.
6. Barskiy, D. A.; Pravdivtsev, A. N.; Ivanov, K. L.; Kovtunov, K. V.; Koptyug, I. V., Simple analytical model for Signal Amplification by Reversible Exchange (SABRE) process. *Phys. Chem. Chem. Phys.* **2015,** *89*, 89-93.
7. Knecht, S.; Pravdivtsev, A. N.; Hovener, J.-B.; Yurkovskaya, A. V.; Ivanov, K. L., Quantitative description of the SABRE process: rigorous consideration of spin dynamics and chemical exchange. *RSC Adv.* **2016,** *6*, 24470-24477.
8. Bernstein, H. J.; Pople, J. A.; Schneider, W. G., The Analysis of Nuclear Magnetic Resonance Spectra: I. Systems of Two and Three Nuclei. *Can. J. Chem.* **1957,** *35* , 67-83.
9. Günther, H., 1H-NMR-Spektren vom AA′ XX′ - und AA′ BB′-Typ – Analyse und Systematik. *Angew. Chem.* **1972,** *84*, 907-920.
10. Günther, H., 1H-NMR Spectra of the AA′XX′ and AA′BB′ Type - Analysis and Classification. *Angew. Chem. Int. Ed.* **1972,** *11*, 861-874.
11. Bantreil, X.; Nolan, S. P., Synthesis of N-heterocyclic carbene ligands and derived ruthenium olefin metathesis catalysts. *Nat. Protoc.* **2010,** *6*, 69-77.
12. Vazquez-Serrano, L. D.; Owens, B. T.; Buriak, J. M., The search for new hydrogenation catalyst motifs based on N-heterocyclic carbene ligands. *Inorganica Chimi. Acta* **2006,** *359*, 2786-2797.
13. Harris, R. K.; Becker, E. D.; Cabral de Menezes, S. M.; Goodfellow, R.; Granger, P., NMR nomenclature. Nuclear spin properties and conventions for chemical shifts (IUPAC Recommendations 2001). *Pure Appl. Chem.* **2001,** *73*, 1795.
14. Markley, J. L.; Bax, A.; Arata, Y.; Hilbers, C. W.; Kaptein, R.; Sykes, B. D.; Wright, P. E.; Wüthrich, K., Recommendations for the presentation of NMR structures of proteins and nucleic acids (IUPAC Recommendations 1998). *Eur. J. Biochem.* **1998,** *256*, 1-15.
15. Theis, T.; Ortiz, G. X.; Logan, A. W. J.; Claytor, K. E.; Feng, Y.; Huhn, W. P.; Blum, V.; Malcolmson, S. J.; Chekmenev, E. Y.; Wang, Q., et al., Direct and cost-efficient hyperpolarization of long-lived nuclear spin states on universal $^{15}N_2$-diazirine molecular tags. *Sci. Adv.* **2016,** *2*, e1501438-e1501438.
16. Logan, A. W. J.; Theis, T.; Colell, J. F. P.; Warren, W. S.; Malcolmson, S. J., Hyperpolarization of Nitrogen-15 Schiff Bases by Reversible Exchange Catalysis withpara-Hydrogen. *Chem. - Eur. J.* **2016,** *22*, 10777-10781.
17. Barskiy, D. A.; Shchepin, R. V.; Coffey, A. M.; Theis, T.; Warren, W. S.; Goodson, B. M.; Chekmenev, E. Y., Over 20%15N Hyperpolarization in Under One Minute for Metronidazole, an Antibiotic and Hypoxia Probe. *J. Am. Chem. Soc.* **2016,** *138*, 8080-8083.
18. Shchepin, R. V.; Barskiy, D. A.; Coffey, A. M.; Theis, T.; Shi, F.; Warren, W. S.; Goodson, B. M.; Chekmenev, E. Y., 15N Hyperpolarization of Imidazole-$^{15}N_2$for Magnetic Resonance pH Sensing via SABRE-SHEATH. *ACS Sens.* **2016**, 640-644.
19. Shchepin, R. V.; Barskiy, D. A.; Mikhaylov, D. M.; Chekmenev, E. Y., Efficient Synthesis of Nicotinamide-1-15N for Ultrafast NMR Hyperpolarization Using Parahydrogen. *Bioconjugate Chem.* **2016,** *27* , 878–882.